



NEW ZEALAND SOCIETY FOR EARTHQUAKE ENGINEERING  
**2019 Pacific Conference on  
Earthquake Engineering**  
TURNING HAZARD AWARENESS INTO RISK MITIGATION  
4 – 6 April | SkyCity, Auckland | New Zealand



---

# A novel connection system for seismic damage avoidance design of moment resisting frames

*S.M. Shabankareh & P. Zarnani*

Auckland University of Technology, Auckland, New Zealand

*A. Hashemi & P. Quenneville*

The University of Auckland, Auckland, New Zealand

## ABSTRACT

Moment-resisting frames are one of the efficient lateral-load resisting systems in terms of providing architectural freedom in design and imposing smaller forces on foundations. Recent major earthquakes have resulted in significant plastic deformations in the beam-column connections causing irrecoverable damage in structures. As a result, engineers have focused on developing new systems which not only provide the life-safety of the residents, but also minimise the damage such that the building could be reoccupied quickly after severe events with minimal business interruption and repair costs.

In this paper, a self-centring damage avoidance concept using the innovative Resilient Slip Friction Joint (RSFJ) is developed for steel Moment Resisting Frames (MRFs). The RSFJ provides the self-centring behaviour as well as energy dissipation in one compact component requiring no post-event maintenance. In this concept, the beam is connected to the column using a pin assembly at top, and the RSFJs acting in tension and compression at bottom. The RSFJs allows for the gap opening in the connection during loading and re-centres the system upon unloading. Furthermore, a secondary collapse-prevention fuse within the RSFJ is considered to keep maintaining a ductile behaviour in the system in case of an event greater than the design earthquake.

Furthermore, in this paper an analytical model is developed to accurately predict the moment-rotation behaviour of this system. The seismic performance of the proposed concept is investigated by full-scale experimental component testing. The test results validate the predictive model and demonstrate the efficiency of this new self-centring system for seismic damage avoidance design of MRFs.

## 1 INTRODUCTION

Seismic structural systems can be classified into categories (Clifton et al. 2010). Category 1 refers to high damage structural design or the conventional steel moment resisting frames.

In this category, fully restrained welded/bolted connections between the beams and columns have been used. Conventional moment frames are designed to dissipate energy under the design earthquake by yielding in the main structural members. That is why the structure is damaged to prevent collapse and yielding in the plastic hinges can lead to significant inelastic deformations in the beams and columns, resulting in permanent structural damage as well as residual story drifts after the earthquake.

Most modern design codes are category 1 systems, as they are based on an estimate of the demand and capacity. Since the plastic deformation generally happens, considerable repairs or replacements might be required after a major earthquake.

Usually, in this method the design provides sufficient detailing to meet the desired performance objectives and plastic deformation is transferred to the pre-defined positions such as reduced beam sections.

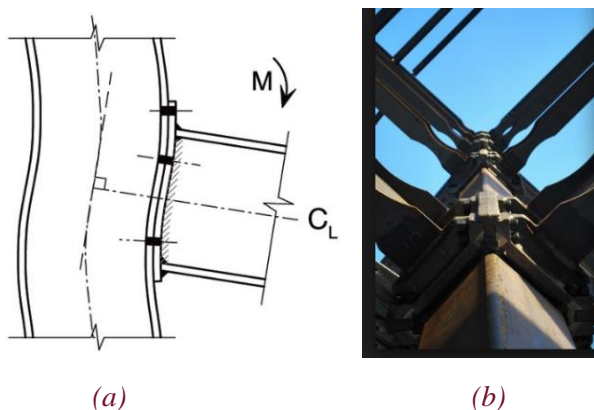


Figure 1: Category 1 – a. conventional method for design MRF, b. Reduced beam section detailing for MRF

Category 2 refers to low damage design. One approach to accomplish this objective is to design the structure to be strong enough to prevent any inelastic/nonlinear action, but this is generally uneconomic in terms of construction costs and maybe less resilient.

After the Northridge earthquake, several research projects were commenced to improve new concepts for steel frames to decrease the onsite working and to avoid inelastic deformations posed by the yielding of the structural elements (Roeder et al. 2000). The application of friction-based energy dissipating devices in steel structures dates back to 1982 when Pall et al. used them in the braced frames to absorb the seismic energy. Clifton et al. (2007 and 2010), introduced the Sliding Hinge Joint (SHJ) as a low damage option alternative to the traditional steel MRFs. The SHJ permits for gap opening in the beam-column contact area and energy dissipation by sliding movement of the plates.

To avoid structural damages and residual drift, post-tensioned beam-column connections for self-centring moment resisting frames (SC-MRFs) were proposed by Ricles et al. (2001). In which the gap opening in the contact zone of the beam-column connection gives the inelastic behaviour and the strands make the self-centring. Later Garlock et al. (2002) proposed an empirical design procedure for steel PT frames based on the design earthquake loads.

This paper introduces a self-centring damage avoidance concept for steel MRFs using the innovative Resilient Slip Friction joint (RSFJ) technology (Zarnani et al. 2015). The RSFJ provides self-centring and energy dissipation through friction in one compact package requiring no post-event structural maintenance.

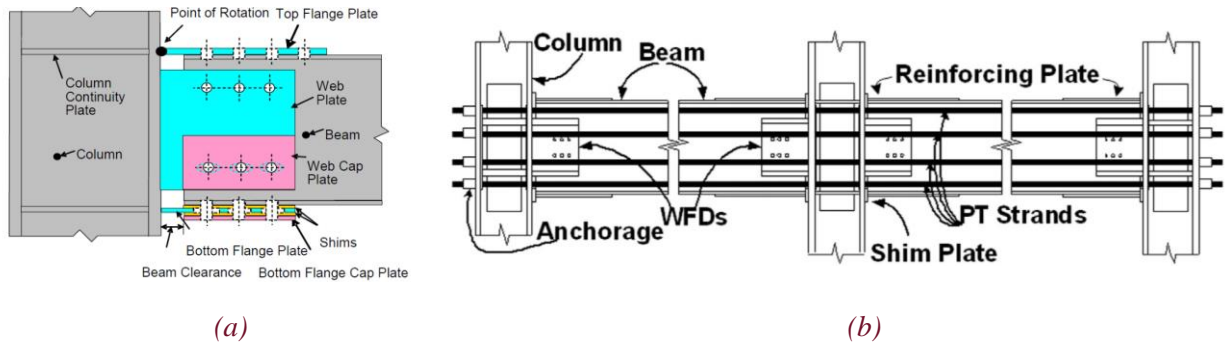


Figure 2: Category 2 – a. Sliding Hinge Joint, b. PT self-centring MRF

## 2 RESILIENT SLIP FRICTION JOINT (RSFJ)

The concept of slip friction joints with the flat steel plates sliding over each other has always been recognized as an effective structural damping solution (Zarnani et al. 2015 and 2016). The energy dissipation mechanism of these joints is one of the most efficient amongst the passive damping technologies.

Nonetheless, the lack of self-centring behaviour in these joints potentially requires the use of another supplementary system, which can be costly, to re-centre the structure to its initial position.

In this paper, a novel friction joint is presented in which the components are formed and arranged in a way that the self-centring behaviour is achieved as well as damping, all in one compact package. Figure 3 shows the components and the assembly for the RSFJ (Hashemi et al. 2016 and 2017). The specific shape of the ridges combined with the use of disc springs provide the required self-centring behaviour. The angle of the ridges is designed in a way that at the time of unloading, the reversing force induced by the elastically compacted disc springs is larger than the resisting frictional force between the sliding plates. Therefore, the elastic force of the discs re-centres the slotted sliding plates to their initial position.

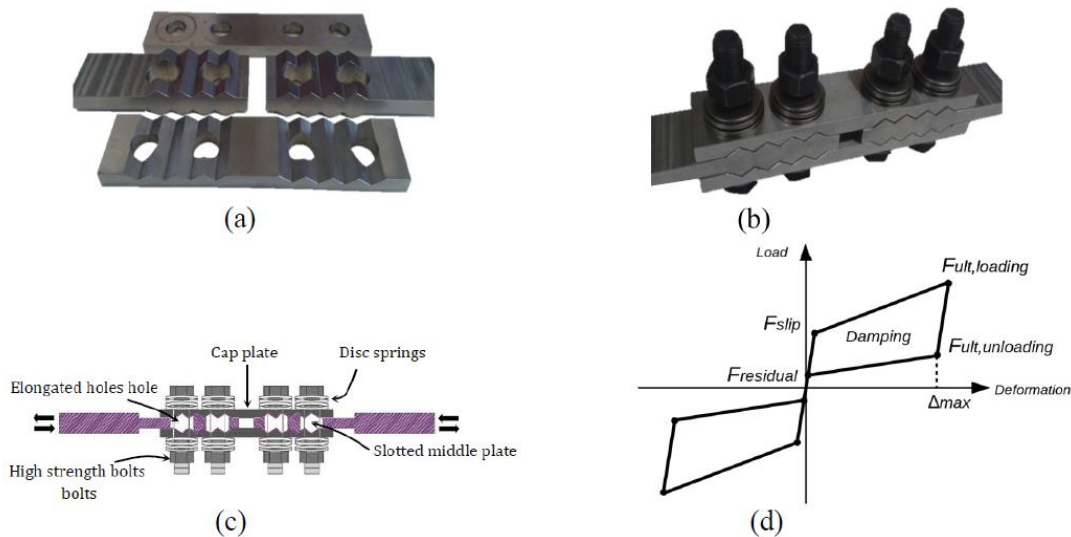


Figure 3: RSFJ: (a) sliding plates (b) assembly (c) components (d) hysteresis

Figure 3 (d) displays the load-deformation behaviour for the RSFJ. The slip force ( $F_{slip}$ ) and the residual force ( $F_{residual}$ ) in the joint can respectively be determined by Eq.1 and Eq.2 where  $F_{b,pr}$  is the clamping force in the bolts,  $n_b$  is the number of bolts,  $\theta$  is the angle of the ridges,  $\mu_s$  is the static coefficient of friction and  $\mu_k$  is the kinetic coefficient of friction. The ultimate force in loading ( $F_{ult,loading}$ ) and unloading ( $F_{ult,unloading}$ ) can be calculated by replacing  $\mu_s$  and  $F_{b,pr}$  in Eq.1 and Eq.2 by  $\mu_k$  and  $F_{b,u}$ , respectively (Zarnani et al. 2015).

$$F_{slip} = 2n_b F_{b,pr} \left( \frac{\sin\theta + \mu_s \cos\theta}{\cos\theta - \mu_s \sin\theta} \right) \quad (1)$$

$$F_{residual} = 2n_b F_{b,pr} \left( \frac{\sin\theta - \mu_k \cos\theta}{\cos\theta + \mu_k \sin\theta} \right) \quad (2)$$

### 3 DAMAGE AVOIDANCE STEEL MOMENT RESISTING FRAMES (MRFS) USING RSFJ

The general concept of damage avoidance steel MRFS with RSFJs is demonstrated in Figure 4. In this idea, the RSFJ is located along the bottom beam flange and consist of two middle plates and two cap plates. The two middle plates (with elongated holes) are attached to the beam bottom flange and the column. The two cap plates are clamped to the middle plates, and friction is generated when the middle plates slide against the cap plates. A pin is used at the top that can transfer the shear forces and axial loads. It should be noted since pure pin have almost zero construction tolerance, a shim plate may be used between connection plate and column's flange.

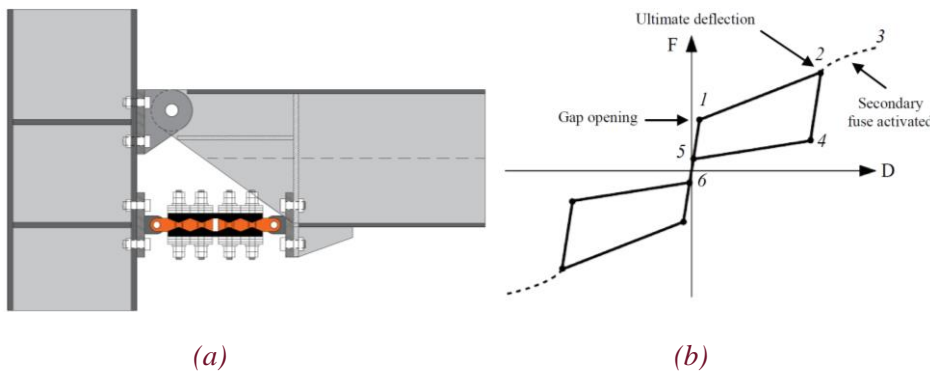
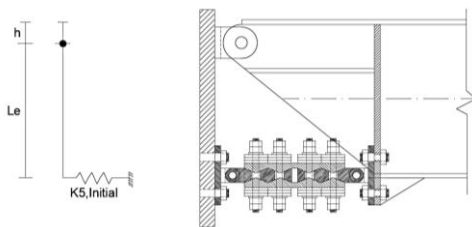


Figure 4: The concept of self-centring MRF with RSFJ: (a) general arrangement (b) theoretical hysteresis

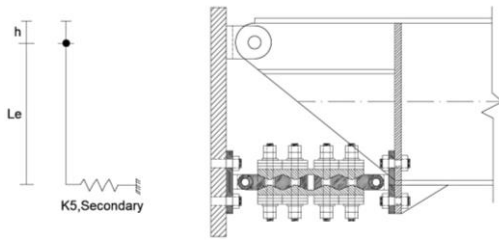
The conceptual relationship between the moment in the beam at the column face  $M$ , and the relative rotation between the beam and the column  $\theta_r$ , is shown in Figure 4 (b). Under the applied loading, the connection has an initial stiffness similar to that of a fully restrained bolted moment connection, where  $\theta_r$  is negligible (before stage 1). In this phase, the elastic stiffness of the RSFJ governs the stiffness of the connection. The beam connection is considered fixed and the stiffness of the entire system depends on beam and column stiffness's. Once the applied moment overcomes the frictional resistance in the RSFJ, rotation and gap opening are imminent (at stage 1). Eq. 3 and Eq. 4 show the moment capacity of the connection at slipping point.



$$M_{slip} = F_{slip} \times L_e = (K_{initial} \times L_e \times \theta_{slip}) \times L_e = (K_{initial} \times L_e^2) \times \theta_{slip} = K_{\theta-initial} \times \theta_{slip} \quad (3)$$

$$K_{\theta-initial} = K_{initial} \times L_e^2 \quad (4)$$

After sliding, the moment capacity of the connection increases because the compaction of the disc springs produces additional axial force. The connection reaches the maximum capacity (stage 2) when the RSFJ reaches the ultimate capacity  $F_{RSFJ,ult}$ . Eq.5 and Eq. 6 show the ultimate moment capacity of the connection at the ultimate gap opening point.



$$M_{ult} = M_{slip} + M_{1-2} \quad (5)$$

$$\begin{aligned} M_{1-2} &= F_{ult-slip} \times L_e = (K_{secondary} \times L_e \times \theta_{ult-slip}) \times L_e = (K_{secondary} \times L_e^2) \times \theta_{ult-slip} \\ &= K_{\theta-secondary} \times \theta_{ult-slip} \end{aligned} \quad (6)$$

Note that if the load in the RSFJ continues to increase to more than  $F_{RSFJ,ult}$ , the secondary fuse can be activated (from stage 2 to stage 3). When the RSFJ reaches its maximum capacity and the ridges are locked, the clamping bolts (or rods) start to yield. The plastic elongation of the rods provides additional travel distance for the joint allowing it to maintain a ductile behaviour up to and even more than the collapse limit state of the structure. This means that when the RSFJ is designed for Ultimate Limit State (ULS) seismic loads (usually corresponds to 2.5% of inter-story drift), a ductile behaviour can be provided up to the Maximum Credible Earthquake (MCE), which is usually close to 4% of inter-story drift.

Upon unloading (from stage 2 to stage 4), the variation in  $\theta_r$  is insignificant. Between stages 2 and 4, moment contribution from the RSFJ changes direction due to a reversal of the friction force, where at stage 4 reversal of the friction force is complete. Between stages 4 and 5,  $\theta_r$  reduces as the beam comes back in contact with the column flange but is under compression. Between stages 5 and 6, the moment decreases to zero as the beam is fully compressed against the column face. A similar moment-rotation behaviour is expected in the opposite direction.

#### 4 COMPONENT TESTS OF THE RSFJ

In order to experimentally investigate the hysteretic behaviour of the RSFJ, a series of joint component tests were conducted. Figure 5 displays the assembly of the manufactured specimen which comprised of two middle slotted plates and two cap plates. All plates were manufactured using mild steel grade 350. The angle of the grooves was 15 degrees. The testing has been conducted using a 100 kN Instron Universal Test Machine with a load cell mounted on the crosshead above the RSFJ prototype to monitor the overall applied force. In order to measure the displacement within the joint, a Linear Variable Differential Transducer (LVDT) device was employed. It should be noted that the measured deflection is the relative displacement between the two slotted centre plates which the loading heads are attached to them.



(a) (b)

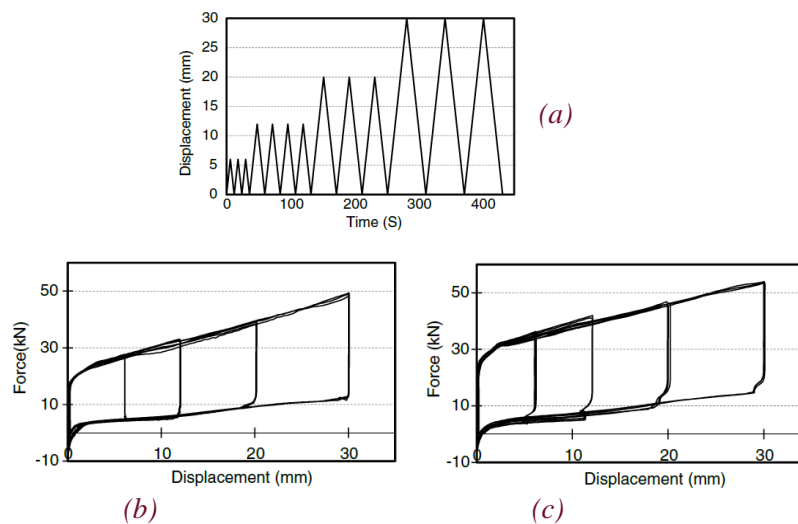
Figure 5: Component test: (a) before slip (b) after slip (Hashemi et al. 2017)

Table 1 presents the design parameters and the capacity of the manufactured RSF joint based on the design procedure described in the previous sections. The slip force ( $F_{slip}$ ) was 24 kN, 31 kN for the tests.

*Table 1: Characteristics of the tested RSFJ*

Parameter	Value	Design Parameter	Value
Angle of the grooves	35	Disc spring thickness (mm)	6.5
Number of bolts ( $n_b$ )	1	Disc spring overall height (mm)	8
$\mu_s$	0.19	Disc spring internal height (mm)	1.5
Slotted whole length (mm)	35	Disc spring outside diameter (mm)	70
Each washer capacity (kN)	110	Disc spring inside diameter (mm)	21
$n_s$ (Per bolt)	9		

From Figure 6(b)–(c), it can be seen that the load-deformation behaviour of the RSFJ represents “flag-shaped” hysteretic curves which imparts the self-centring behaviour as well as a significant rate of energy dissipation.



*Figure 6: RSFJ component test results (Hashemi et al. 2017): a) The applied displacement schedule b) Hysteretic behaviour for  $F_{slip} = 24$  kN c) Hysteretic behaviour for  $F_{slip} = 31$  kN*

These results suggest that RSF technology has a high potential for the application in seismic resistant structures specially when a resilient damage avoidant design is required in order to protect the structures from major seismic events and the associated aftershocks.

## 5 NUMERICAL MODELLING OF THE STEEL MRFS WITH RSFJS

This section briefly describes the numerical modelling and analysis of steel MRFs with RSFJs.

The flag-shaped hysteresis of the RSFJ can be modelled using ABAQUS finite element software, SAP2000 and ETABS providing the design parameters are properly calibrated. To study the behaviour of the RSFJs, a prototype joint is considered. Input data shows the specifications of the joint including the geometric

properties, friction coefficient and specification of the disc springs. These analytical results showed that in the proposed model, flag shaped behaviour of the joint completely matched with experimental results.

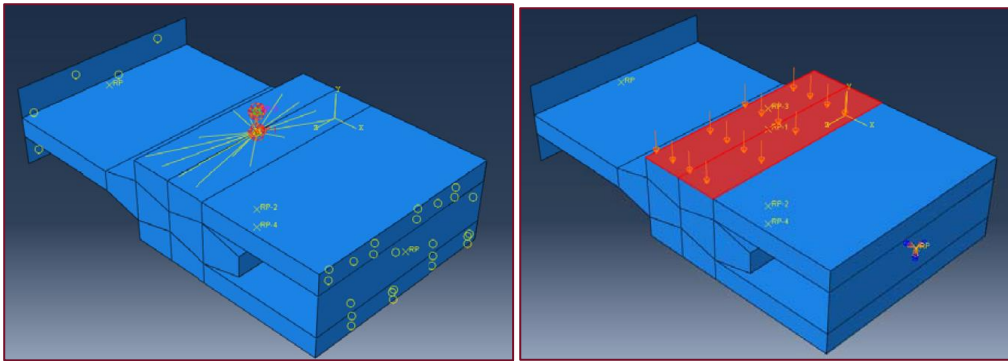
### 5.1 Modelling in ABAQUS:

For modelling of RSFJ in ABAQUS (Hibbitt et al. 2014) the steps below should be followed. The result showed that theoretical and analytical hysteresis curves are complied.

Step1. Input data, input parameter for this model is same to component test (Table 1)

Step2. Modelling, in this step half of the joint assembly has been modelled to optimize the analysis time.

Step3. Define bolt, discs and pre-pressure, spring option in the software can be used for modelling of the bolt and discs' stiffness (Figure 7 (a)). Pre-pressure can be defined as an area load (Figure 7 (b)).



(a)

(b)

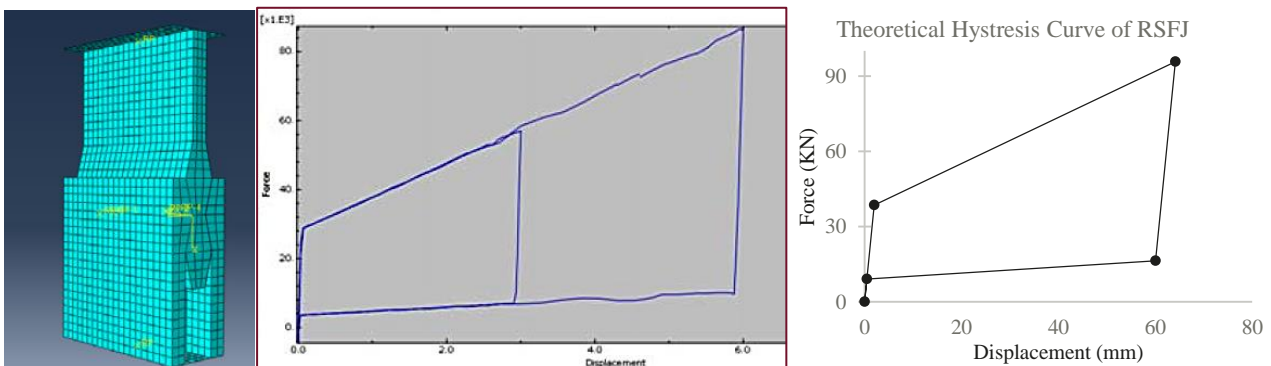
Figure 7: RSFJ modelling in ABAQUS: (a) Defining washers' stiffness (b) Defining pre-pressure

Step5. Define the cyclic displacement, two cycles of displacement equal to 30mm and 60 mm have been defined in ABAQUS.

$$D = V \times t \text{ (time step = 0.1s)} \rightarrow D_1 = 1 \times 0.3 \times 0.1 = 0.03 \text{ m}, D_2 = 1 \times 0.6 \times 0.1 = 0.06 \text{ m} \quad (7)$$

Step6. Define the contact friction, friction should be defined as a tangential behaviour. In the Interaction module of the software, "All with self" should be selected so that friction is considered between all surfaces in contact.

Step7. Final step is defining mesh for the model (Figure 8 (a)) and performing the analysis (Figure 8 (b)).



(a)

(b)

(c)

Figure 8: (a) Defining mesh (b) Analysis result in ABAQUS (c) Theoretical hysteresis curve

## 5.2 Modelling in SAP2000:

The RSFJ can be easily integrated in the structural analysis and design programs ETABS and SAP2000 (CSI 2011). It allows the designer to accurately calibrate the parameters according to the requirements of the project. In ETABS/SAP2000, the RSFJ can be modelled using the “Damper – Friction Spring” link Element. This function accurately represents the flag-shaped hysteresis of a RSFJ provided its parameters are properly calibrated in accordance with the design parameters of the joint. The parameters can be defined for any of the six translational or rotational degrees of freedom [16].

The design parameters of the RSFJ are,  $F_{slip}$  (slip force of the RSFJ),  $F_{ult}$  (ultimate force in the RSFJ at the end of loading),  $F_{restoring}$  (restoring force of the RSFJ),  $F_{residual}$  (residual force in the RSFJ at end of unloading),  $\Delta_{slip}$  (initial elastic deflection of the RSFJ before slip),  $\Delta_{ult}$  (ultimate displacement of the RSFJ),  $K_{initial}$  (initial stiffness of the RSFJ before slip),  $K_{loading}$  (loading stiffness of the RSFJ) and  $K_{unloading}$  (unloading stiffness of the RSFJ).

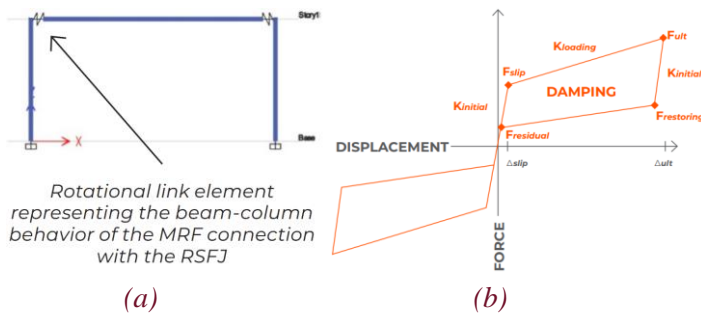


Figure 9: (a) SAP2000 modelling (b) Design parameters

The recommended approach to model the MRFs with RSFJs is to model the moment-rotation behaviour of the beam-column connection using a single link element. The link element can be attached to the beam and column in their contact interface. The moment-rotation behaviour of the MRF connection can be specified respecting the force in the RSFJ ( $F_{RSFJ}$ ) and the lever arm ( $L_e$ ) which is the vertical distance between the centre of the RSFJ and the rotating pivot close to the top beam flange. For this case, the parameters should be defined for the related rotational degree of freedom (for example,  $R3$  when in the global “XZ” plane). The other five degrees of freedom should be “fixed”. The active direction should be defined as “Both” given the link element works in both directions.

Damper – Friction Spring design parameters:

- Initial (Non-slipping) Stiffness =  $K_{\theta-initial} = K_{initial} \times L_e^2$
- Slipping Stiffness (Loading) =  $K_{\theta-loading} = K_{secondary} \times L_e^2$
- Slipping Stiffness (Unloading) =  $K_{\theta-unloading} = K_{unloading} \times L_e^2$
- Pre-compression displacement =  $(-M_{slip}) / K_{\theta-loading} = - [(K_{initial} \times L_e^2) \times \Theta_{slip}] / [K_{secondary} \times L_e^2] = - (K_{initial} / K_{secondary}) \times \Theta_{slip}$
- Stop displacement =  $\Theta_{ult}$

By defining these parameters, the rest of the RSFJ parameters ( $\Theta_{slip}$ ,  $M_{ult}$ ,  $M_{restoring}$  and  $M_{residual}$ ) will be automatically adjusted.

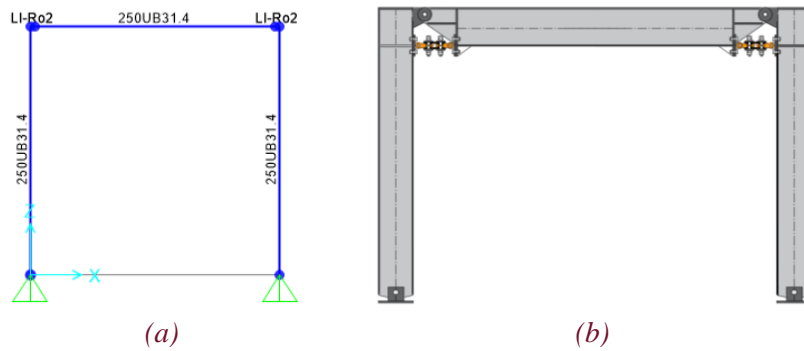


Figure 10: (a) SAP2000 model (b) Position of RSFJ in MRF

To study the behaviour of the steel MRFs with RSFJs, a prototype frame is considered. Figure 10 (a) shows the specifications of the frame including the geometric properties and the frame sections. The frame has 4m, 3m width and height respectively and the columns are pinned to the foundation.

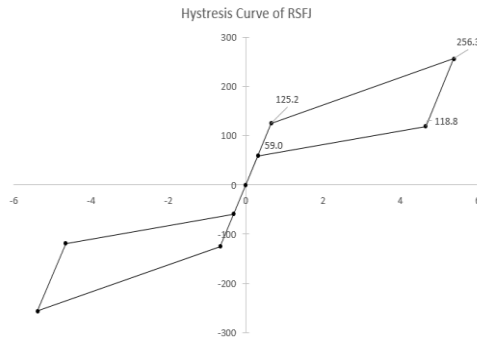
Table 2: Summary of the input data and design parameters for RSFJ

Input Parameter	Value	Design Parameter	Value
Angle of the grooves	35	Initial Stiffness (kN/mm)	7.6e6
$n_b$	1	Slipping Stiffness (Loading)	1.1e6
$\mu_s$	0.19	Slipping Stiffness (Unloading)	0.55e6
$F_{b,pr}$ (kN)= 50% $F_{b,ult}$	61	Pre-compression displacement	2.2%
Each washer capacity (kN)	135	Stop displacement (Rad)	2.5%
$n_s$ (Per bolt, each side)	2		

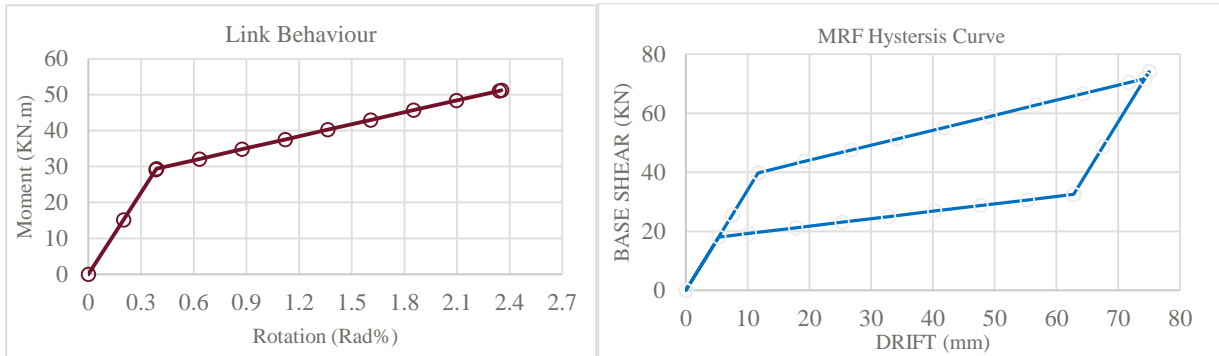
The required ULS moment capacities for the connections were determined as 50 kN.m. The slip threshold for the RSFJs is specified as 50% of the ULS moment capacity. Table 2 shows the input data and the calculated design parameters for the MRF connections.

Push-over simulations were carried out for the frame with RSFJ. RSFJs were used for all of the connections.

Figure 11 (a) displays the moment-rotation curve for one of the connections. The Figure 11 (b) shows the base shear and the maximum story drift. It can be seen that the MRF connection shows a flag-shaped hysteresis with a fully re-centring behaviour.



(a)



(a)

(c)

Figure 11: (a) Theoretical hysteresis curve of RSFJ (b) Link behaviour (c) Hysteresis curve of MRF

## 6 TEST SETUP

In order to verify the performance of the moment connection with RSFJ, a prototype test is planned (see Figure 12(a)). The RSFJ has been designed for ultimate load of 350 kN (Figure 12(b)). The beam and connection have been designed based on NZS 3404 and ultimate moment equal to 500 kN.m since behaviour of RSFJ after ultimate force (secondary fuse phase) also will be considered. It should be noted that by increasing the number of bolts (in RSFJ) or length of lever arm (size of beam), larger capacity could be achieved.

In this test, RSF joint has totally four bolts and each bolt has three disc springs at each side. Angle of the grooves is 25 degree and pre-compressing force of discs is 61 kN. The connection will be tested for 450 kN.m moment.

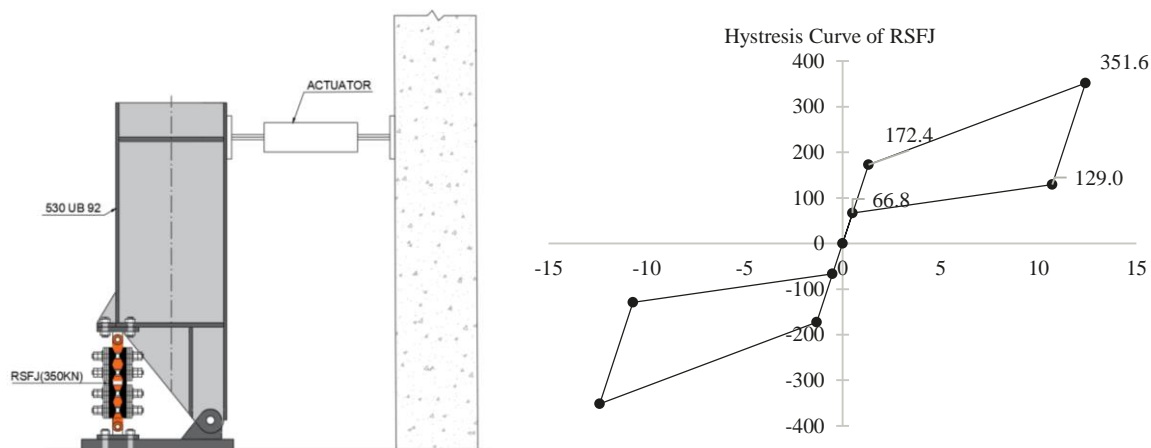


Figure 12: (a) MRF test setup with RSFJ (b) predicted hysteresis curve of RSFJ

## 7 CONCLUSIONS

This paper introduced the concept of damage avoidance self-centring steel Moment Resisting Frames (MRFs) using innovative Resilient Slip Friction Joints (RSFJs). In this concept, the RSFJ is connected to the bottom flange of the beam and the required ductility is provided by the gap opening in the beam-column contact surface. This connection offers a flag-shaped moment-rotation relationship demonstrating the self-centring behaviour. Furthermore, a secondary fuse within the RSFJ is introduced to prevent any brittle failure in the connection even when the applied force is higher than the design seismic load. The behaviour of the secondary fuse is verified by experimental tests.

In addition, numerical simulations on a one-story steel frame demonstrated the seismic performance of the proposed system. Overall, the findings of this research confirmed an excellent seismic performance in terms of stability and self-centring behaviour.

## 8 REFERENCES

- Clifton, G.C., MacRae, G.A., Mackinven, H., Pampanin, S. & Butterworth, J. 2007. Sliding hinge joints and subassemblies for steel moment frames, *Proc of New Zealand Society for Earthq Eng Conf*, Palmerston North, New Zealand.
- Clifton, G.C., MacRae, G.A., Mackinven, H., Mago, N., Butterworth, J. & Pampanin, S. 2010. The sliding hinge joint moment connection, *Bull. New Zeal. Soc. Earthq. Eng.*, Vol 43(3) 202.
- Computers and Structures, Inc. 2011. *SAP2000: Structural Analysis Program*, USA.
- Garlock, M. 2002. *Full-Scale testing, seismic analysis, and design of post-tensioned seismic resistant connections for steel frames* [Ph.D. dissertation]. Bethlehem, PA: Dept. of Civil and Environmental Engineering, Lehigh University.
- Hashemi, A., Masoudnia, R. & Quenneville, P. 2016. A numerical study of coupled timber walls with slip friction damping devices, *Constr. Build. Mater.*, Vol 121 373–385.
- Hashemi, A., Masoudnia, R. & Quenneville, P. 2016. Seismic performance of hybrid self-centring steel-timber rocking core walls with slip friction connections, *J. Constr. Steel Res.*, Vol 126 201–213. *Key Engineering Materials*, Vol 763 733
- Hashemi, A., Loo, W.Y., Masoudnia, R., Zarnani, P. & Quenneville, P. 2016. Ductile Cross Laminated Timber (CLT) Platform Structures with Passive Damping, *World Conference of Timber Engineering WCTE2016*, Vienna, Austria.
- Hashemi, A., Zarnani, P., Masoudnia, R. & Quenneville, P. 2017. Seismic resistant rocking coupled walls with innovative Resilient Slip Friction (RSF) joints, *J. Constr. Steel Res.*, Vol 129 215–226.
- Hashemi, A., Zarnani, P., Masoudnia, R. & Quenneville, P. 2017. Seismic resilient lateral load resisting system for timber structures, *Constr. Build. Mater.*, Vol 149 432–443.
- Hashemi, A., Zarnani, P., Masoudnia, R. & Quenneville, P. 2017. Experimental testing of rocking Cross Laminated Timber (CLT) walls with Resilient Slip Friction (RSF) joints, *J. Struct. Eng.*, Vol 144(1) 4017180-1-16.
- Hibbitt, K. 2014. *ABAQUS*. Standard User's Manual. V. 6.13
- Pall, A.S. & Marsh, C. 1982. Response of friction damped braced frames, *J. Struct. Eng.*, Vol 108(9) 1313–1323.
- Roeder, C.W. & Venture, S.A.C.J. 2000. *State of the art report on connection performance*, SAC Joint Venture.
- Ricles, J.M., Sause, R., Garlock, M. & Zhao, C. 2001. Post-tensioned seismic-resistant connections for steel frames, *J Struct Eng*, Vol 127(2) 113–21.
- Zarnani, P. & Quenneville, P. 2015. *A resilient slip friction joint*, Patent No. WO2016185432A1, NZ IP Office
- Zarnani, P., Valadbeigi, A. & Quenneville, P. 2016. Resilient slip friction (RSF) joint: A novel connection system for seismic damage avoidance design of timber structures, *World Conf. on Timber Engineering WCTE2016*, Vienna Univ. of Technology, Vienna, Austria.